PREVENTIVE AND EMERGENCY TRANSIENT STABILITY CONTROL

Damien Ernst*, **Daniel Ruiz-Vega, Mania Pavella**
University of Liège, Sart-Tilman B28, B - 4000 Liège, Belgium
Mania.Pavella@ulg.ac.be

* Research Fellow, FNRS

Abstract: A unified approach to transient stability closed-loop control is presented. It relies on the general transient stability method called SIME, from which the Preventive and the Emergency SIMEs are derived. The Preventive SIME uses time-domain simulations of plausible contingencies prior to their occurrence, for the on-line power system monitoring from the control room. The Emergency SIME, on the other hand, uses real-time measurements, acquired on the system power plants after the actual occurrence of a contingency in order to appraise and trigger countermeasures indispensable for the system integrity. Despite fundamental differences in their design and objectives, the two approaches have also common features. This paper highlights main differences and similarities, and illustrates them on a realistic, large power system. The tradeoff between on-line preventive control and real-time emergency control is also assessed in terms of size of the involved countermeasures.

Keywords: Transient stability assessment and control; closed-loop control; on-line preventive control; real-time closed-loop emergency control; SIME method.

1 INTRODUCTION

Power system transient stability control is as important as problematic an issue. Important, since control is the ultimate objective of any security study, be it static or dynamic. Problematic, since it implies appraisal of appropriate type and size of countermeasures.

Conventional time-domain transient stability methods cannot handle such tasks. Direct methods are better suited; but they lack flexibility with respect to power system modelling, stability scenarios, and types of instability. Hybrid methods are more appealing, since a priori they are capable of combining advantages of both.

Broadly, two classes of hybrid methods may be distinguished, namely, those relying on multimachine Lyapunov functions and those using generalised one-machine equivalents. The popular TEF method is of the former class (e.g., see [1,2]), the SIME method belongs to the second class [3,4].

This paper presents a SIME-based unified approach to closed-loop transient stability preventive and emergency controls.

Preventive control in general aims at assessing "what to do" in order to avoid the system loss of synchronism if an a priori harmful contingency *would occur*. Its design relies on stability simulations of this contingency scenario. More precisely, *on-line preventive control* aims at setting up in a horizon of, say, 30 minutes ahead, means to stabilize the system if it were threatened by any of the plausible contingencies found to be harmful. For a given (or forecasted) operating condition, this task may be accomplished by computing stability margins of harmful contingencies, and designing appropriate countermeasures. The decision about whether to execute or postpone such actions relies on engineering judgement about the tradeoff between economics and security.

Emergency control, on the other hand, aims at triggering a countermeasure in real time, after a harmful contingency *has actually occurred*. This action may be either designed in real time using real-time measurements, or assessed in anticipation by means of off-line stability simulations. The latter case belongs to **open-loop emergency control**, as opposed to **closed-loop emergency control**; in this latter case, the action *is designed and triggered in real time, during the transient period following contingency inception, and the system continues being monitored and further controlled*. In emergency situations the necessity to call upon automatic control actions becomes vital for both security and economics.

This paper deals with a general framework of closed-loop controls, encompassing preventive and emergency modes. They both use the SIME method, which initially was developed to improve the performances of the conventional time-domain approach to transient stability assessment [4]. Later on, this method has been extended to cover preventive and emergency control aspects; this yielded the “Preventive SIME” and the “Emergency SIME”. The Preventing SIME goes well beyond the conventional way of thinking and opens avenues to a large variety of new applications (e.g., see [5,6]). On the other hand, the Emergency SIME departs definitely from the traditional simulations-based approaches, by processing real-time measurements after the actual occurrence of a contingency to control *predictively* the power system [7,8]. This paper aims to give a unified view of the preventive and the emergency closed-loop controls, to point out salient common features as well as fundamental differences. At the same time, the paper aims to test the Emergency SIME on meshed power system structures, in addition to radial structures investigated so far [7,8].

The paper is organized as follows. Section 2 outlines essentials of the SIME approach to transient stability assessment (TSA) in general, then focuses on the differences between preventive and predictive TSA. Section 3 deals with the two modes of closed-loop control: preventive control, using preventive TSA, and emergency control, using predictive TSA. In both cases the considered countermeasures concern machines’ active generation power. Section 4 illustrates the above two modes on the 88-machine EPRI test system C [9]. Among the reported simulation results of particular interest is the variation of the amount of controlled power necessary to stabilize a system vs the “control time”, i.e. the time elapsed between the contingency inception and the control action.

2 TRANSIENT STABILITY ASSESSMENT BY SIME

2.1 SIME method in general

SIME is a hybrid method which replaces the trajectories of a multimachine power system by the trajectory of an one-machine infinite bus (OMIB) equivalent. This OMIB results from the multimachine decomposition into two groups of machines, the aggregation of each one of these latter into an equivalent machine, and finally the replacement of these two machines by an OMIB. The OMIB parameters are inferred from those of the system machines, while its identification and stability properties

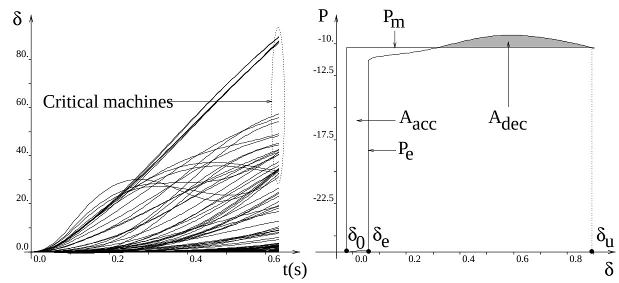

(a) Swing curves

(b) OMIB equal-area criterion (EAC)

Figure 1. Principle of SIME’s TSA: illustration on the stability case of Section 4

are inferred from the equal-area criterion (EAC). OMIB parameters and stability properties are refreshed at the rate of acquisition of the multimachine parameters.

More precisely, for a given unstable scenario, SIME proposes to EAC a few number (say 5) of candidate OMIBs; in turn, EAC chooses that candidate which first meets its instability conditions [4]:

$$P_a \;=\; P_m - P_e \;=\; 0 \;\; ; \;\; \dot{P}_a > 0 \, . \qquad (1)$$

It then declares this OMIB to be the relevant one and recognizes the machines’ decomposition into “critical” and “non-critical” ones. Further, it computes the corresponding (unstable) margin

$$\eta \;=\; A_{dec} - A_{acc} \;=\; -\int_{\delta_0}^{\delta_u} P_a d\delta \;=\; -\frac{1}{2} M \omega_u^2 \, . \quad (2)$$

Figure 1 illustrates the above descriptions in the real-world stability case of Section 4, simulated in the preventive mode; the contingency is a 3-ϕ short-circuit cleared at $t_e = 100$ ms by opening one line. More specifically, Fig. 1a displays the multimachine swing curves up to the “time to (reach) instability”, t_u ; this is the time where the instability conditions (1) are met. (Here, $t_u = 635$ ms.) The first OMIB to reach these conditions is made of 32 critical machines (CMs) and 56 $(88-32)$ non-critical machines (NMs). It is interesting to note that of the 32 CMs, a first group of 7 machines is significantly more advanced from the remaining 25 ones than these latter from the NMs; indeed, the angular distance between the less advanced of the 7 machines and the more advanced of the 25 machines is about 32°, whereas the angular distance between the last CM and the first NM is of 3.8°. Figure 1b displays the OMIB $P-\delta$ representation in terms of P_m and P_e . The normalized stability margin, η/M , computed according to (2), equals -1.044 (rad/s)^2.

2.2 Acronyms and notation

2.2.1 General

In the above descriptions and throughout the remainder of the paper, the following acronyms and notation are used.

EAC : equal-area criterion
OMIB : one-machine infinite bus
TSA : transient stability assessment
CM : critical machine
NM : non-critical machine

A_{acc} (A_{dec}) : accelerating area (decelerating area) in the $P-\delta$ plane
$P_a = P_m - P_e$: OMIB accelerating power, excess of its mechanical power, P_m, over its electrical power, P_e
d : (angular) distance or difference between two successive machines, sorted in decreasing order of their angles; in the context of the Preventive SIME d is measured at t_u
M : OMIB inertia coefficient
t_u : time to (reach) instability, i.e. time where the unstable conditions (1) are met
$\delta_e(t_e)$: clearing angle (time)
δ_0 (δ_u) : OMIB initial angle (angle at t_u)
ω_u : OMIB speed at t_u
η : margin; η/M : normalized margin
P_c (ΔP_c) : total active power of the CMs (variation of P_c).

2.2.2 Specific to the Emergency SIME

$t_0 = 0$: beginning of the during-fault period
t_e : beginning of the post-fault period (here :100 ms)
Δt : time sample, i.e. time between two successive measurement sets acquisition (in Section 4, $\Delta t = 20$ ms)
t_f : time relative to the first set measurements acquisition (here :135 ms)
t_i : current processing time
t_c : control time, i.e., time elapsed between a contingency inception and the control action
t_d : time delay between measurements' processing, and control's application
$\delta_i = \delta(t_i)$: OMIB angle at t_i
$\omega_i = \omega(t_i)$: OMIB speed at t_i.

2.3 Preventive vs Emergency SIME

According to its principle SIME combines information about the multimachine power system with the EAC stability assessment of the OMIB.

Depending upon whether the multimachine information is obtained from transient stability simulations or from measurements acquired on the system power plants in real-time, yields the Preventive or the Emergency SIME.

Both SIMEs aim at performing successively two main tasks: transient stability assessment and control. But while the Emergency SIME attempts to control the system *just after* a contingency occurrence and its clearance, so as to stabilize it in time, the Preventive SIME aims at proposing countermeasures *preventively*, i.e. *before* any contingency occurrence.

2.3.1 Preventive transient stability assessment

Preventive TSA goes along the traditional way of assessing the system robustness vis-à-vis occurrence of anticipated contingencies. In an on-line context, preventive TSA should consider all plausible contingencies, in a horizon of, say, 30 minutes ahead: computational efficiency becomes thus crucial.

On-line preventive TSA may effectively be decomposed into contingency filtering, to detect existence of harmful contingencies while discarding the (large majority of) harmless ones, and assessment of these harmful contingencies, in particular of their degree of severity.

According to SIME, these tasks are achieved using time-domain simulations to determine stability margins and critical machines [4,5,10]. The resulting filtering and ranking procedures are significantly faster than those relying on conventional pure time-domain approaches. Nevertheless, the paramount advantage lies in the possibility of assessing margins and critical machines, which open avenues to control. This issue is addressed in Section 3 and illustrated in Section 4.

2.3.2 Predictive transient stability assessment

Unlike to the preventive TSA, the predictive TSA has not been used so far, for two main reasons: on one hand, because this task is hardly achievable - if at all - by conventional approaches; on the other hand, because its interest is directly linked to the feasibility of closed-loop emergency control - and, again, this cannot be handled by conventional approaches.

Unlike to the Preventive TSA, the predictive TSA deals, in real-time, with an event (or succession of events) which has been detected but not necessarily identified, and generally automatically cleared by the protective devices. Thus, in order to be effective, it must *predict* the system behaviour *early enough* so as to leave sufficient time for determining and triggering appropriate control actions, whenever necessary. To get a stability diagnostic ahead of time, the predictive TSA relies on real-time measurements.

More precisely, the method predicts the stability of the system entering its post-fault configuration, i.e. *after* the disturbance inception and its clearance, using the multi-machine data available at successive time samples Δt's (e.g., 1 sample every 20 ms). Thus, at each time sample, an OMIB analysis is performed to decide whether the system keeps stable or is driven to instability. The crux for this analysis is the prediction of the OMIB $P_a - \delta$ curve, and hence the prediction of the unstable angle, δ_u, and corresponding stability margin. The achievement of the prediction brings out the following two questions:

1. which are the most disturbed machines ?
2. is the system driven to (in)stability and to what extent ?

Answers to these questions rely on the following steps, illustrated in Figs 2.[1]

(i) At a time t_i short after the disturbance clearance, $(t_i \geq t_e + 2\Delta t)$ consider the incoming measurements at times $t_i - 2\Delta t$, $t_i - \Delta t$, t_i, and use Taylor series to predict the individual machine angles at some time ahead (e.g. 100 ms). Sort the machines in decreasing order of these angles and consider as candidate critical machines those advanced machines which are above the largest (angular) distance (see notation, § 2.2).

(ii) Construct the corresponding OMIB, determine its parameters $(\delta, \omega, \gamma, P_a)$ from the corresponding parameters of the individual power plants at times $t_i - 2\Delta t$, $t_i - \Delta t$, t_i, and approximate the $P_a - \delta$ curve by solving the expression:

$$P_a(\delta) \approx a\delta^2 + b\delta + c \tag{3}$$

for a, b, c at these times.[2]

(iii) Solve eq. (3) to find the OMIB angle $\delta_u > \delta(t_i)$ which verifies conditions (1).

(iv) Compute the stability margin, η, according to (2):[3]

$$\eta = -\int_{\delta_i}^{\delta_u} P_a d\delta - \frac{1}{2} M\omega_i^2 \,. \tag{4}$$

(v) If η is found to be negative or close to zero, declare the system to be unstable and determine control actions (see Section 3).

[1] Figure 2a sketches the principle, while Fig. 2b illustrates its application to the real case simulated in Section 4. Notice that the curves in Fig. 2b are drawn after the disturbance clearance. (Actually, they start being drawn 10 time samples after t_f, the first acquisition of measurement set.)

[2] Among various possible extrapolation techniques, the least squares technique shows to be particularly robust.

[3] Expression (4) is equivalent to but more appropriate than (2), since it relies on the already computed P_a curve.

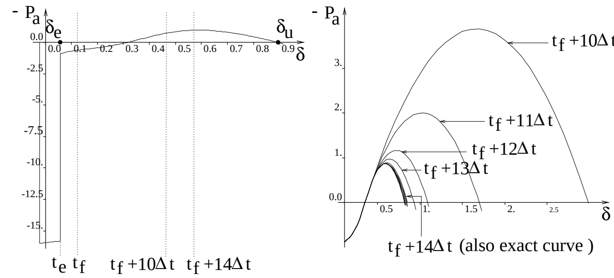

(a) General description

(b) application to the stability case of Section 4

Figure 2. Principle of the predictive TSA

(vi) In this latter case, compute the *time to instability*, t_u, i.e. the time for the OMIB to reach its unstable angle, δ_u, i.e. to go unstable. This may be computed, for example, by [11]:

$$t_u = t_i + \int_{\delta_i}^{\delta_u} \frac{d\delta}{\sqrt{\frac{2}{M}\int_{\delta_i}^{\delta} -P_a d\delta + \omega_i^2}} \tag{5}$$

where δ_i stands for $\delta(t_i)$ and ω_i for $\omega(t_i)$.

(vii) In any case, acquire a new set of measurements and continue monitoring the system.

Remark

Obviously, the above predictive stability assessment relies on two main approximations.

- First, the OMIB used here might not necessarily be the critical OMIB which would be identified at t_u, i.e. when the OMIB actually reaches its unstable angle, δ_u; however, it is likely to contain (part of) the most disturbed machines and certainly machines whose control will (hopefully) stabilize the system.
- Second, the $P_a - \delta$ curve relies on a measurement-based prediction rather than accurate computation. But its accuracy may be assessed by observing that, by definition, for a fixed clearing time t_e the margin (4) should be constant whatever t_i; hence, the margin values obtained at successive t_i's should converge to a (nearly) constant.

Figure 2b shows that the $P_a - \delta$ prediction converges towards the exact $P_a - \delta$ after about 14 time samples after the first prediction; this corroborates what Table 2 of Section 4 shows: the value of η stabilizes around 435 ms.

Further comments

1.- Computationally, the above strategy is extraordinarily unexpensive and fast; indeed, at each time sample, it merely requires (a) solving the individual Taylor series to identify the OMIB; (b) computation of the OMIB parameters and of the P_a curve (3); (c) solving it to get δ_u ; (d) computing the margin (4). Obviously, all these computations require only fractions of ms.

2.- The time to instability, t_u , expressed by (5) is a good indicator of the contingency severity; moreover, it provides valuable advice about whether to act immediately, though imperfectly, or to wait for a more accurate assessment.

3.- It may happen that the transient stability phenomena take some time to get organized, and do not appear clearly enough at the beginning of the post-fault transients, thus yielding a confused diagnostic. However, in such cases instability is likely to develop rather slowly; this leaves time to continue monitoring until the phenomena become clearer. (See Table 2 of Section 4.)

4.- Along the same lines, a case which at the first time instants yields a stable margin may actually be unstable. It is therefore advisable to continue monitoring the system for about one second before declaring it definitely stable.

5.- The above developments assume that the individual power plant, variables may be obtained by synchronized phasor measurement devices placed at each power plant together with some local processing power to determine generator angles, speeds and accelerations.

3 CLOSED-LOOP CONTROL

3.1 General principle

Transient stability control relies on the following two propositions:

- the instability of a multi-machine power system is measured by the OMIB margin;
- stabilizing an unstable case consists of canceling out this margin, i.e. of increasing the decelerating area and/or decreasing the accelerating area in the OMIB $P-\delta$ plane (see Fig. 1b).

  Broadly, this may be achieved:

  – either by reducing the mechanical power of the OMIB[4] and hence of the CMs.[5] E.g., by using fast-valving, generator shedding, generator rescheduling, etc.;
  – or by increasing the electrical power. E.g., by using braking resistors, DC links, thyristor controlled series compensators, and other FACTS.

[4] unless back-swing phenomena are of concern, in which case the CMs' power should be increased.

[5] Indeed, it can be shown that $\Delta P_{OMIB} = \Delta P_{CM}$ [6].

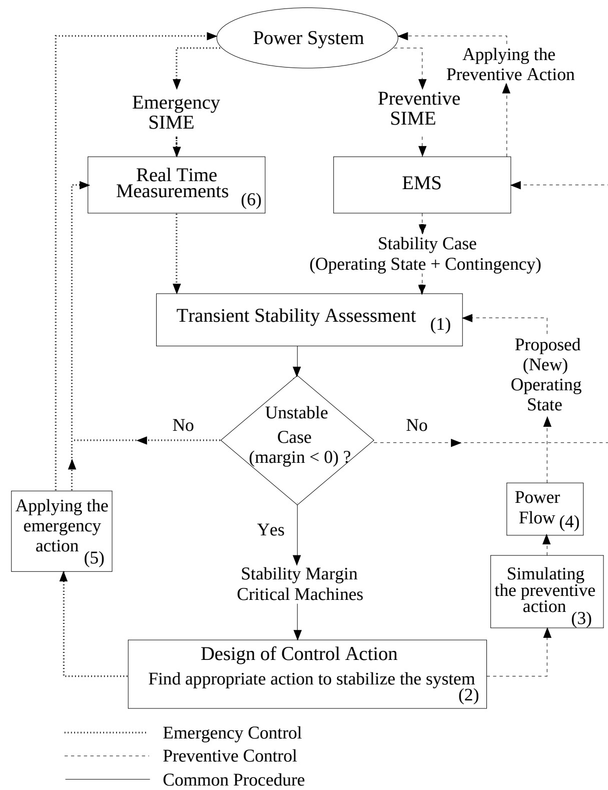

Figure 3. General framework for transient stability closed-loop control. Taken from [12].

The above principle yields the closed-loop control framework portrayed in Fig. 3.

This general framework is applied below to the particular case where the control consists of reducing the mechanical power of the CMs; according to the mode of control, this yields generation rescheduling (preventive countermeasure) or generation shedding (emergency countermeasure).

More specifically, cancellation of the (negative) margin η_0 is obtained through the general iterative procedure sketched in Fig. 4 and commented hereafter:

(i) determine a decrease rate ΔP_{c0} of P_{c0} , where P_{c0} is the total active generation of CMs yielding η_0

(ii) using $P_{c1} = P_{c0} - \Delta P_{c0}$, re-run the stability case and compute the new margin, η_1

(iii) extra/inter-polate linearly η_0, η_1 to get a first-guess

(iv) according to the size and sign of η_1 , decide whether P_{cLim} may be deemed accurate enough to stop or to continue iterating.

The above iterative pattern is shown to be robust and fast for both preventive and emergency controls, despite many important differences in its application to one or the other mode. In anticipation, we mention the following main differences:

- in the preventive mode, the generation decrease on CMs must be compensated by an (almost) equal increase on non-critical machines, in order to meet the desired consumption.[6] This compensation is not realized in the context of emergency control (at least at the first instants following this control)
- the way of assessing the amount of generation decrease
- the way of assessing the operating conditions resulting from the generation decrease on CMs
- in the emergency mode, the generation decrease on CMs is often made stepwise (shedding discrete generation quantities by disconnecting units, as is the case for hydro power plants); in the preventive mode the generation decrease may be continuous
- a priori, the total amount of generation which must be removed from CMs to stabilize an unstable case is expected to be significantly larger in the emergency mode than in the preventive one. This is mainly due to the delay in applying the control. Figure 6 in Section 4 illustrates this aspect.

All these differences are discussed below and illustrated in Section 4.

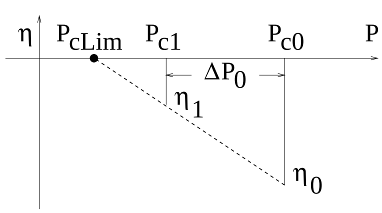

Figure 4. Principle of the iterative control procedure

[6]This condition cannot be met always, though.

3.2 Preventive control

Preventive control relies on the iterative procedure mentioned in § 3.1 and illustrated in Fig. 4. Note that, as already mentioned, in the preventive mode the generation decrease on CMs must be compensated by an (almost) equal generation increase on NMs. This leaves many degrees of freedom in the way of distributing the power decrease on CMs, and of reporting (almost) equivalent increase on NMs. Generally, SIME takes care of CMs' rescheduling while an OPF program may take care of NMs rescheduling [5,6]. This allows meeting different objective functions such as transient stability-constrained congestion management, or ATC calculations. Ref. [13] elaborates on such issues.

Table 1 illustrates the closed-loop preventive control on the case considered in Section 4 and described in Fig. 1. The iterative procedure starts with an unstable (normalized) margin $\eta_0 = -1.044$; it corresponds to a total CMs' generation of $24,623$ MW. After reducing this power by 3 % ($\Delta P_{c0} = -739$; $P_{c1} = 23,884$ MW), a power flow is performed, followed by a stability run which yields a positive margin $(\eta_1 = 1.072)$. Linear interpolation of η_0 , η_1 yields $P_{cLim} = 24,258$ MW . The simulation may be stopped or pursued, depending upon the accuracy sought. Note that the actual value is of 24,183 MW. Thus, according to the above computation, to stabilize the considered contingency scenario, the CMs generation must be decreased by 365 (actually by 440) MW, i.e., by about 1.5 % (1.8 %). Note that the above stabilization has been obtained by decreasing the power of the 7 most advanced CMs, proportionally to their inertia. (Remember, there are 32 CMs, see description of § 2.1, and Section 4.) Other, additional stabilization patterns are considered in Section 4, yielding countermeasures.

Table 1. Closed-loop preventive control

1	2	3	4	5	6	7
Iter. Nr	η/M (rad./s)^2	Nr of CMs	P_{ck} (MW)	ΔP_{ck} (MW)	P_{ck+1} (MW)	t_{obs} (ms)
0	-1.044	32	24,623	-739	23,884	635
1	1.072	32	23,884	Int.	24,258	5,000

3.3 Emergency control

3.3.1 General considerations

For unstable scenarios and corresponding negative margins, the question of concern is: which corrective actions should be taken to satisfactorily stabilize the system ?

To answer this question, first remember that a negative margin means that the decelerating area in the $P_a - \delta$ plane is not large enough.

Further, observe that there is always an additional time delay, t_d, before actually triggering the corrective action; it corresponds to the sum of three terms, viz.:

- the time needed to receive the real-time measurements[7],
- the time to transmit the order to the power plant(s),
- the time to apply the corrective action.[8]

Observe that the longer the time delay, the larger the size of the corrective action (amount of generation power to be shed). This is corroborated by Fig. 6 in Section 4.

Existence of this delay makes also more difficult the handling of real-time measurements when designing control actions. Indeed, for a period of t_d s after the corrective action has been taken, the incoming measurements refer to the uncontrolled system, while what actually matters is the behaviour of the controlled system. This issue is addressed below.

3.3.2 Generation shedding assessment

In the particular case of generation shedding, the generators to be shed are chosen among the critical ones. The concern is to appraise the amount of generation to be shed. Subsequently, i.e. after the corresponding control order has been sent to the generator plant, it is important to continue refining the assessment, using new real-time measurements. The purpose is to assess whether the generation shedding already assessed is indeed sufficient or, otherwise, how much additional generation to shed. Obviously, because of the transmission delays, one should anticipate the changes introduced by the control, based on information gathered prior to this control.

To determine how many generators to shed, Ref. [8] proposes an approximative expression of the "controlled" margin in terms of the number of generators shed and solves for the latter so as to yield a positive margin.

The prediction relies on the following assumptions:

– the mechanical power of the individual machines is not affected by the generation shedding, during the short time frame considered
– the remaining machines will take over the electrical power initially generated; this amounts to neglecting the increase in the equivalent transient and transformer reactances, thus leading to optimistic errors; if the number of generators shed is small with respect to the total number in operation and if the transmission lines are long, this approximation error will however be negligible.

[7] since measurements concerning the system at time t_i are received with some delay.

[8] All in all, t_d could be about 150 ms.

Thus, the "indirect" procedure for determining the number of generators to shed consists of computing the "controlled margin" for decreasing numbers of generators in the controlled system.

Another possibility is provided by a direct computation, also proposed in [8]; this also relies on acceptable assumptions, which, however, underestimate the benefit of the control action.

Whether direct or indirect, the closed-loop emergency control, and more generally the emergency SIME follows the pattern described below.

1. OMIB identification
2. Prediction of the $P_a - \delta$ curve
3. Computation of δ_u
4. Computation of η.

   The above 4 steps are described in § 2.3.2.
5. Assessment of the number of generators to shed
6. Checking the accuracy of η: repeat above steps (1) to (4) for successive t_i's to check whether the successive η values converge to a constant, as they should (see Remark of § 2.3.2) or to continue further
7. Checking the effectiveness of the corrective action: similarly, repeat step 5 with refreshed parameter values to assess whether the generation shedding has indeed stabilized enough the power system or whether to shed more.

4 SIMULATIONS

4.1 Simulations description

The simulations are performed on the EPRI test system C, having 434 buses, 2357 lines and 88 machines (of which 14 are modelled in detail) [9]. The considered base case has a total generation of 350,749 MW.

The contingency considered in both the preventive and the emergency approaches is a 3-ϕ short-circuit applied at bus #15 (500 kV); it is cleared 100 ms after its inception, ($t_e = 100$) by opening the line 1-15.

In the preventive mode, SIME is coupled with the ETMSP program [14]. This program is also used in the emergency mode, in order to create artificially real-time measurements, since such measurements are not available.

4.2 Preventive SIME

Part of the simulation results have already been reported in previous sections 2.1, 3.2. They are collected below, together with additional ones.

Simulation conditions : $t_0 = 0$ (contingency inception); $t_e = 100$ ms ;

Simulation results of the preventive TSA: $t_u = 635$ ms (see Fig. 1a); $\eta_0 = -1.044$ (rad/s)^2 ;

Simulation results of the preventive control: number of CMs : 32; of them, 7 are significantly more advanced than the remaining 25 ones, with respect to the group of NMs : the angular distance of the former is 32° vs 3.8° for the latter (see § 2.1); total power generated by the CMs : $P_{c0} = 24,623$ MW .

To stabilize this scenario, various patterns may be considered, depending on the way of reporting on CMs the power decrease. 6 different patterns are considered below. Their iterative procedure has the common start, indicated in Table 1, which is $\Delta P_{c0} = -0.03\, P_{c0} = -739$ MW . These patterns along with the corresponding total power decrease on CMs are summarized as follows.[9]

- Power decrease on the 7 more advanced CMs, proportionally to their inertia. Assessed by SIME after 1 iteration: 365 MW (see Table 1); actual value: 440 MW.
- Power decrease on the 7 more advanced CMs, equally reported on these machines: 440 MW.
- Power decrease on the 32 CMs proportionally to their inertias: 980 MW.
- Power decrease on the 32 CMs, proportionally to the product $d_i * M_i$: 705 MW. [10]
- Power decrease on the first more advanced CM (machine 1877): 430 MW.

Note that whenever possible the corresponding power increase on NMs is equally reported on NMs.

Observe the existence of significant differences of the total power decrease of various patterns. Observe also the many possibilities suggested in the choice of machines to control, and the corresponding possibilities for performing transient stability-constrained congestion management, ATC calculations and the like.

[9] A detailed account of patterns of power system distribution on CMs is given in the companion paper [13]. Note that the contingency scenario used here differs slightly from that of contingency 1 used in [13]; contingency clearing time : 95 ms vs 100 ms; contingency clearance : by tripping line 5-15 vs line 1-15.

[10] d_i denotes the angular distance of the i-th CM with respect to the most advanced NM, and M_i its inertia coefficient.

4.3 Emergency SIME

The simulations of the predictive TSA are displayed in Fig. 2b. On the other hand, Table 2 summarizes the results of both predictive TSA and closed-loop emergency control.

Simulation conditions : $t_0 = 0$ (contingency inception); $t_e = 100$ ms ; first set of data: acquired at $t_f = 135$ ms ; rate of data acquisition: $\Delta t = 20$ ms .

Simulation results of the predictive TSA : the predictive TSA computations start at $t_i = 135 + 2 \times 20 = 175$ ms (remember, three measurement sets are necessary for running the predictive TSA (§ 2.3.2)).

Table 2. Closed-loop emergency control

1	2	3	4	5
t_i (ms)	δ_u (rad.)	t_u (ms)	η/M (rad/sec)^2	η/M after shedding
375	1.094	788	-0.60	
395	0.922	676	-0.81	
Corrective decision is taken (3 units shed)				
415	0.850	631	-0.88	0.271
435	0.822	614	-0.91	0.115
455	0.813	610	-0.91	0.092
475	0.820	617	-0.91	0.113
495	0.826	622	-0.90	0.151
515	0.836	631	-0.90	0.234
535	0.850	642	-0.89	0.347
555	0.858	649	-0.89	0.376
Corrective action is applied				
575	0.861	652	-0.89	0.352
595	0.860	652	-0.89	0.361
615	0.859	651	-0.89	0.373
635	0.861	652	-0.89	0.384

At the beginning (175 ms up to 375 ms), the simulations do not provide a clear prediction (identification of CMs and corresponding margin): it seems as though the system is not going to lose synchronism. But at $t_i = 375$ ms (i.e., $t_f + 13\,\Delta t$) the first unstable margin appears along with the corresponding group of CMs: this group is composed of 33 machines, of which the 32 are those identified by the Preventive SIME. Table 2 summarizes the sequence of events from 375 ms onwards. Observe that the predicted time to instability is quite short: around 670 ms, at $t_i = 395$ ms , i.e., less than 300 ms later. This is why a corrective action is decided before waiting for the margin to converge to a constant value, which is (nearly) reached at $t_i = 435$ ms .

Figure 2b illustrates the above descriptions; it also suggests that:

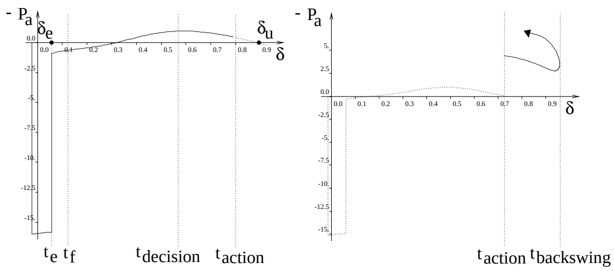

(a) OMIB constructed with 33 CMs (uncontrolled, unstable system)

(b) OMIB constructed with 30 CMs (controlled, stabilized system)

Figure 5.

- there is no margin before $t_i = 375$ ms ($= t_f + 12\,\Delta t$)
- the prediction starts being reliable around 435 ms ($= t_f + 14\,\Delta t$) ; indeed, the P_a–δ curve drawn at 435 ms is found to coincide with the "exact" curve, obtained by the preventive SIME.

It is interesting to compare results of the preventive and predictive TSA:

- the time to instability, t_u , is found to be of 635 ms by the preventive SIME, whereas the predictive TSA yields values varying between 788 ms (at $t_i = 375$ ms) and 614 ms (at $t_i = 435$ ms);
- the normalized margin is found to be of -1.044 (rad/s)^2 by the preventive TSA, whereas the predictive TSA underestimates it slightly (around -0.9 by the predictive TSA).

Simulation results of the emergency control: because of the proximity to instability, it is decided to take control action quite early (at $t_i = 415$ ms). The type of action is shedding CMs; the size of this action, assessed according to § 3.3, is found to be the 3 units among the 7 more advanced ones, corresponding to 2,463 MW.[11]

Table 2 summarizes the sequence of the events.

• Let us first focus on columns 2 to 4 which refer to the monitoring of the system, relying on the incoming measurements at the rate of 20 ms: rows $t_i = 415$ to 555 ms correspond to the measurements of the uncontrolled system; they suggest that the predicted loss of synchronism reaches good accuracy (the margin value stabilizes around -0.90 (rad/s)^2) and that it is imminent: the t_u value stabilizes around 640 ms. At $t_i = 575$ ms , i.e. 160 ms after the control decision has been taken, the control (generators' shedding) is actually triggered. But for 3 additional samples, up to $t_i = 635$ ms , the incoming measurements still refer to the uncontrolled system due to the communications delay (supposed to be of 50 ms).

• Consider now column 5 of the table which refers to the controlled system, i.e. to the system evolution after the shedding of 3 units. They are all predicted results: rows corresponding to $t_i = 415$ up to 555 ms) predict the system evolution as will be after the control triggering, whereas row $t_i = 575$ ms assesses the system evolution after the control triggering.

Observe that the negative margin of column 4 stabilizes to a more constant value than the positive margin of column 5; this is due to the fact that the negative margin relies on a correct expression (eq. (2) or (4)), whereas the positive margin results from an approximate expression [4].

Figure 5 describes the sequence of the closed-loop control events: the control decision is taken at $t_i = 415$ ms (corresponding to an angle of about 0.57 rad), relying on stability conditions where the number of CMs is 33. The control starts acting at $t_i = 555$ ms. It is sufficient to stabilize the system : the $P_a - \delta$ curve experiences a return angle of about 0.93 rad; it corresponds to $t_r = 975$ ms .

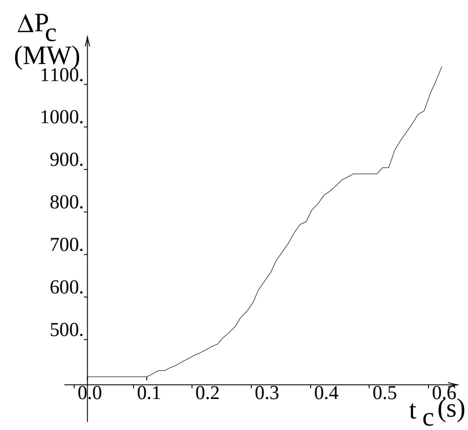

Figure 6.

4.4 Variation of control size vs control time

It was suggested earlier that the total generation change (decrease) on CMs, ΔP_c , necessary to stabilize a system subject to a contingency, is likely to depend on the "time to control", t_c , i.e. the time elapsed between the contingency inception and the actual control action.[12]

[11] The machines shed are 1875 (835 MW), 1771 (793 MW) and 1877 (835 MW).

[12] An interesting discussion on preventive vs corrective countermeasures can be found in [15]

The ΔP_c vs t_c curve has been computed on the contingency scenario considered in this section: first in the preventive mode (one value), then in the emergency mode, where simulations are performed every 10 ms (totalling 60 simulations). The resulting curve is displayed in Fig. 6 and commented below.

- All ΔP_c values are obtained by distributing equally the generation decrease on the 7 more advanced CMs. Note that the time-domain program decreases proportionally these machines' inertia coefficients and synchronous reactances. The resulting ΔP_c values are thus slightly overestimated. This, however, does not change the general trend of the curve.
- The ΔP_c of the preventive mode is given at $t_c = 0$ and equals 399 MW; actually it was computed about 15 s earlier, in order to avoid that transients spoils the result.

5 CONCLUSION

This paper has considered and compared two approaches to transient stability control: the Preventive and the Emergency SIMEs. They both process information about the multimachine power system to get an one-machine equivalent, and thus to compress information and extract synthetic transient stability assessment and and control. But while the Preventive SIME uses time-domain simulations of contingencies prior to their occurrence, to appraise corresponding preventive countermeasures, the Emergency SIME uses real-time measurements following the actual occurrence of a contingency, to appraize corrective countermeasures indispensable for the system integrity. The size of countermeasures is significantly more important for the corrective, emergency mode than for the preventive mode; but preventive actions might be considered too costly, given the generally low probability of contingencies' occurrence. A good tradeoff might be found from the combination of the two types of actions. In terms of feasibility, the Preventive SIME is now sufficiently mature for its on-line application. On the other hand, the Emergency SIME, relies on technological challenges, which however, are about to be overcome.

6 REFERENCES

[1] *Power System Transient Stability Analysis Using the Transient Energy Function Method*, A.A. Fouad and V. Vittal. Prentice-Hall Inc., 1992.

[2] *Energy Function Analysis for Power System Stability*, M.A. Pai. Kluwer Academic, 1989.

[3] "Generalized One-Machine Equivalents in Transient Stability Studies", M. Pavella. *PES Letters, IEEE Power Engineering Review*, Vol.18, No.1, January 1998, pp. 50-52. See also Ref. [3] therein.

[4] "SIME: A hybrid approach to fast transient stability assessment and contingency selection", Y. Zhang, L. Wehenkel, P. Rousseaux and M. Pavella. *Int. Journal of Electrical Power and Energy Systems*, Vol.19, No.3, 1997, pp. 195-208.

[5] "Transient Stability-Constrained Maximum Allowable Transfer", L. Bettiol, L. Wehenkel and M. Pavella. *IEEE Trans. on Power systems*, Vol.14, No.2, May 1999, pp. 654-659.

[6] "Transient stability-constrained generation rescheduling", D. Ruiz-Vega, A.L. Bettiol, D. Ernst, L. Wehenkel and M. Pavella. *Bulk Power System Dynamics and Control IV - Restructuring*, Santorini, Greece, Aug. 1998, pp. 105-115.

[7] "A method for real-time transient stability emergency control", Y. Zhang, L. Wehenkel and M. Pavella. *Proc. of CPSPP'97, IFAC/CIGRE Symp. on Control of Power systems and Power Plants*, Beijing, China, Aug. 1997, pp. 673-678.

[8] "Real Time Transient Stability Emergency Control of the South-Southeast Brazilian System", D. Ernst, A. Bettiol, Y. Zhang, L. Wehenkel and M. Pavella. *SEPOPE*, Salvador, Brazil, May 1998, (Invited paper, IP044; 9 pages).

[9] *Standard Test Cases for Dynamic Security Assessment*, Final EPRI report No. EPRI TR-105885, Electric Power Research Institute, Project 3103-02-03, December 1995.

[10] "A contingency filtering, ranking and assessment technique for on-line transient stability studies", D. Ruiz-Vega, D. Ernst, C. Machado Ferreira, M. Pavella, P. Hirsch and D. Sobajic. To be presented at the DRPT2000 Conference, London, UK, April 2000.

[11] "Closed-loop transient stability emergency control", Damien Ernst and Mania Pavella. To be presented at the panel session "On-line Transient Stability Assessment and Control"; *IEEE/PES Winter Meeting*, Singapore.

[12] "A general framework for transient stability assessment and control", M. Pavella, D. Ernst and D. Ruiz-Vega. *PES Letters, IEEE Power Engineering Review*, vol.19, No.10, October 1999.

[13] "Preventive countermeasures for transient stability-constrained of power systems", D. Ruiz-Vega, D. Ernst, C. Bulac, M. Pavella, P. Hirsch and D. Sobajic. VII Symposium of Specialists in Electric Operational and Expansion Planning, SEPOPE 2000, 21-26 May 2000, Curitiba Brazil.

[14] "Extended transient midterm stability program version 3.1 User's manual". Final EPRI Report No. EPRI TR-102004, Electric Power Research Institute, Projects 1208-11, 12-13 May, 1994.

[15] Taylor, C. W.:"The Future of On-line Security Assessment and Wide Area Stability Control". To be presented at the panel session "On-line transient stability assessment and control", IEEE PES 2000 Winter Meeting Singapore, January 23 to 27, 2000.

Acknowledgements: The financial support of the Electric Power Research Institute (project WO#3103-10) for performing transient stability investigations on the EPRI system is gratefully acknowledged.